Displacement and stress distribution in the temporomandibular joint during clenching

Kunishige Nagahara, DDS, PhD; Satoru Murata, DDS, PhD; Shoji Nakamura, DDS, PhD; Tomoyuki Tsuchiya, DDS, PhD

Abstract: The aim of this study was to analyze biomechanical reactions in the mandible and TMJ during clenching under various restraint conditions. A three-dimensional finite element model of the mandible, including the TMJ, was created for test purposes. The results were as follows: (1) Under any restraint conditions, displacement was greatest on the surface of the condyle and less on the articular disc and the surface of the glenoid fossa, in that order. Resultant stresses followed the same trend. (2) Displacement and stress were greatest when the lower central incisor was restrained and attenuated as the posterior teeth were restrained. Because the biomechanical reaction of the TMJ during clenching was greatest when the lower central incisor was restrained, premature contact of these teeth may be one of the factors involved in the initiation of temporomandibular arthrosis.

Key Words: Stress analysis, Temporomandibular joint, Clenching, Finite element analysis

The return to prominence of the concept of internal derangement of the temporomandibular joint (TMJ) has contributed greatly to the treatment of TMJ dysfunction. However, the cause of dislocation of the articular disc, which is one of the pathologies of internal derangement of the TMJ, has yet to be clarified.

Hypotheses for the etiology of articular disc dislocation can be divided into two groups: those that take into account loading of the TMJ[1-3] and those that consider traction in the anterior direction generated by hyperstrain of the superior head of the lateral pterygoid muscle.[4,5] The latter theories, in which hyperstrain of the lateral pterygoid muscle causes dislocation of the disc, have recently been refuted based on the results of a detailed anatomical study of the TMJ.[6] At present, the primary cause of dislocation is believed to be aggravation of the biological environment of the TMJ.[7,8] However, only a few biomechanical studies of the TMJ have been conducted using methods such as Strengage,[9] measurement of intra-articular synovial pressure,[10,11] and finite element analysis.[7,12] Although the use of Strengage or measurement of TMJ synovial pressure provide data on pressure and distortion in regions to which the measurement apparatus is attached, distortion and displacement inside the bones cannot be determined. Furthermore, such methods are associated with a variety of problems, including potential harm to the human body and the inconvenient size and low accuracy of the measurement apparatus.

In order to analyze a continuous object numerically, it is essential to approximate infinite freedom of the object to a finite freedom, such that the characteristics of the body are not lost. Finite element analysis is one such method.[13-16] It is not affected by the type and size of the material and circumstances,[14] and it has been applied in many different fields.

In finite element analysis, the normal stress (s_{norm}) works in the normal (vertical) direction of the plane. A positive (+) value indicates a tensile stress and a negative (-) value indicates a compression stress. Each principal stress has a degree and a direction. Thus, describing

Author address
Kunishige Nagahara, DDS, PhD
2-11 Suemori-dori, Chikusa-ku
Nagoya, 464 -8651, Japan,
Kunishige Nagahara, assistant professor, Department of Orthodontics, Aichi-Gakuin University School of Dentistry, Division of Oral Morphology, Research Institute of Advanced Oral Science, Nagoya, Japan.
Satoru Murata, private practice, Toyohashi, Japan.
Shoji Nakamura, assistant professor, Department of Orthodontics, Aichi-Gakuin University School of Dentistry, Nagoya, Japan.
Tomoyuki Tsuchiya, professor and chairman, Department of Pediatric Dentistry, Aichi-Gakuin University School of Dentistry, Division of Oral Morphology, Research Institute of Advanced Oral Science, Nagoya, Japan.

Submitted: April 1998, **Revised and accepted:** October 1998
Angle Orthod 1999;69(4):372-379.

the three-dimensional direction is difficult, and only a few studies of the TMJ using the three-dimensional finite element method (3-D FEM) have been reported.[8,13]

The objectives of the present study were to construct a model of the TMJ using 3-D FEM, and to use that model to biomechanically analyze and compare stresses within the TM joint in response to clenching.

Materials and methods

A dry adult human skull with normal occlusion was examined. The skull was attached to a computed tomography (CT) scanner with the auriculo-infraorbital (Frankfort) plane parallel to the machine, then scanned in 2 mm thick sections from the lower edge of the mandible to the glenoid fossa of the temporal bone. A scanning image of identical size was made.

Next, the shapes of the cortical bone, cancellous bone, lower teeth, and articular disc of each section were projected. The anatomical structure of the articular disc with anterior and posterior bands and intermediate zone was constructed in a section about 2 mm thick, using utility wax.

Each node was digitized and the origin of the coordinate axes was set at the center of the foramen magnum. The Y-axis was set along the median palatine suture, and the anterior direction was set as the + direction. The X-axis was set perpendicular to the Y-axis, and the lateral side set as the + direction. Z-axis values were entered in advance according to the thickness of each section.

Next, the two-dimensional data were used to establish regions and prepare elements of each section. These processes were performed using Fast Medical Meshing software (Yokogawa Techno-information Service Inc, Chiba, Japan). Based on the output file, a 3-D FEM model was developed using COSMOS/M (Structural Research & Analysis Co, Los Angeles, Calif). Because we assumed the model was symmetrical, only the right side of the image was analyzed. The total number of nodes was 40,136, the total number of quadrilateral 8-node solid elements was 31,879, and the total degrees of freedom was 120,408 (Figure 1).

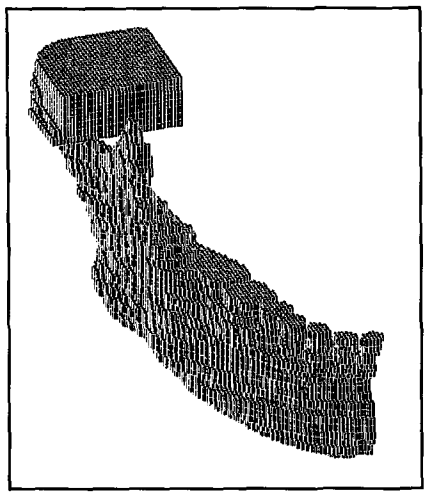

Figure 1
3-D FEM model of the human mandible including the TMJ

The mechanical constants of the elements were determined by reference to Tanaka,[8] as indicated in Table 1.

Finally, loading and restraint conditions were determined. For loading conditions, the traction of the superficial and deeper parts of the masseter muscle, the anterior and posterior parts of the temporalis muscles, and the lateral and medial pterygoid muscles were determined. It was assumed that the magnitude of traction was proportional to the area of the section. Traction was 37.5 N for the superficial part of the masseter muscle and 50.5 N for the deeper part, 71.0 N for the anterior part of the temporalis muscle and 41.5 N for the posterior part, 5.5 N for the lateral pterygoid muscle and 44.0 N for the medial pterygoid. Total traction for the left and right was determined to be 500 N, which is in agreement with the value determined by Tanaka[8] and Tanaka et al.[13] The direction of action of each masticatory muscle was also determined to match those reported by Tanaka[8] and Tanaka et al.[13]

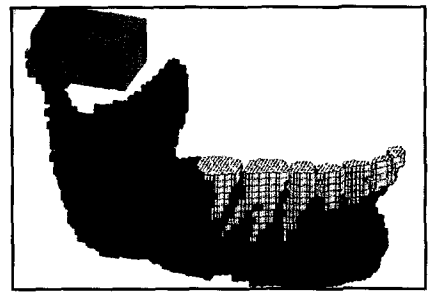

Figure 2
3-D FEM model of the human mandible showing each element

Table 1
Mechanical properties of different components of the model

Component	Elastic modulus (MPa)	Poisson's ratio
Cortical	1.4×10^4	0.30
Cancellous	7.9×10^3	0.30
Teeth	3.0×10^4	0.30
Articular disc	4.4×10	0.40

From Tanaka[8]

For restraint conditions, the upper part of the glenoid fossa of the temporal bone (which is believed not to have a significant effect on the stress of the TMJ[17]) and lower teeth were restrained individually, followed by the restraint of all teeth together.

Method of evaluation

For evaluation of the condyle, disc, and glenoid fossa, the origin was set at the center of the medial and lateral poles of the condyle (Figure 2). Ten nodes on each of the coronal and sagittal plane sections were evaluated.

The nodes were categorized into five groups for evaluation. Three nodes that included the origin were labeled *middle* nodes, four anterior

nodes were labeled *anterior*, four posterior nodes were labeled *posterior*, four medial nodes were labeled *medial*, and four lateral nodes were labeled *lateral*. Mean and standard deviations were calculated for each group.

The stresses derived by finite element analysis are maximum principal stress, median principal stress, and minimum principal stress (abbreviated s_1, s_2, and s_3, respectively). The relationships between these three types of principal stresses and s_{norm} and s_r can be described by the following equations:[18]

$$s_{norm} = s_1 + s_2 + s_3 / 3$$

$$s_r = \sqrt{s_1^2 + s_2^2 + s_3^2 / 3}$$

To evaluate stress analysis, normal and resultant stresses (hereafter referred to as s_{norm} and s_r) were calculated from three principal stresses: maximum, median and minimum principal stresses.

To evaluate displacement analysis, total displacement $\sqrt{x^2+y^2+z^2}$ was calculated from displacement on the X-axis (displacement in mediolateral direction), Y-axis (displacement in anteroposterior direction), and Z-axis (displacement in inferosuperior direction).

Results

Normal stress (Table 2)

For the surface of the condyle (Figure 3A-B), compression stress attenuated in the frontal, middle, lateral, and medial parts as the posterior teeth were restrained. Compression stress ranged between 0.35 and 6.27 KPa, with anterior > middle ≅ medial > lateral, regardless of the restraint conditions. In contrast, stretching stress increased in the posterior nodes under conditions of total tooth restraint.

For the articular disc (Figure 3C-D), compression stress was noted in all regions. Compression stress attenuated as the posterior teeth were restrained and reached a minimum under total tooth restraint. Compression stress ranged between 0.23 and 4.46 KPa, with middle > posterior ≅ lateral > anterior > medial, regardless of the restraint conditions.

For the posterior part of the glenoid fossa (Figure 3E-F), tensile stress was observed under all the restraint conditions, with middle > lateral > anterior. Compression stress occurred in other parts of the glenoid fossa. However, in the medial nodes, the level of compression stress attenuated as the posterior teeth were restrained.

Resultant stress (Table 3)

For the surface of the condyle (Figure 4A-B), resultant stress attenuated as the posterior teeth were restrained and reached a minimum under conditions of total tooth restraint. Stress ranged between 1.03 and 9.78 KPa, with anterior > middle > posterior > medial > lateral, regardless of the restraint conditions.

For the articular disc (Figure 4C-D), resultant stress attenuated as the posterior teeth were restrained and reached a minimum under total tooth restraint. Stress ranged between 0.49 and 6.67 KPa, with middle > lateral > posterior ≅ medial > anterior.

For the glenoid fossa (Figure 4E-F), resultant stress attenuated as the posterior teeth were restrained and reached a minimum level under the conditions of total tooth restraint. Stress ranged between 0.30 and 5.08 KPa, with middle > lateral ≅ posterior ≅ medial > anterior, regardless of the restraint conditions.

The average resultant stress (s_r) for the mediolateral direction was 1.38 KPa for the condyle surface, 0.93 KPa for the articulation disc, and 1.11 KPa for the surface of the glenoid fossa of the temporal bone. The average for the anteroposterior direction was 2.12 KPa for the condyle surface, 0.76 KPa for the articulation disc, and 0.70 KPa for the surface of the glenoid fossa of the temporal bone.

Total displacement (Table 4)

For the condyle surface (Figure 5A-B), total displacement attenuated as the posterior teeth were restrained and reached a minimum under total tooth restraint. Displacement ranged between 0.06 and 0.33 μm, regardless of the restraint conditions, with lateral > anterior ≅ posterior ≅ middle > medial.

For the articular disc (Figure 5C-D), total displacement attenuated as the posterior teeth were restrained and reached a minimum under conditions of total tooth restraint. Displacement ranged between 0.02 and 0.23 μm, with lateral > posterior > middle ≅ anterior > medial, regardless of the restraint conditions.

For the glenoid fossa (Figure 5E-F), total displacement was observed only in the posterior nodes. In the posterior region, displacement attenuated as the posterior teeth were restrained and reached a minimum under total tooth restraint. Displacement ranged between 0.01 and 0.08 μm.

Discussion

Equivalency of model to human body

The accuracy of finite element analysis can be influenced by the type and number of elements. In this study, only the right side of the image was analyzed in the symmetrical model. Because the elements are finely divided, the finite element model is the equivalent of the model of the human body.[14] The following guidelines should be considered when dividing the model into elements:

1. Important regions should be divided into finer elements.
2. Sudden changes in the level of fineness should be avoided.
3. Elements should be divided at regular intervals.

Table 2
Normal stress distributions at each node

Component	Restraint	Anterior	Middle	Posterior	Lateral	Medial
Condyle	Mand 1	-6.27 ± 4.04	-2.65 ± 1.51	0.34 ± 5.06	-0.96 ± 0.52	-2.18 ± 2.27
	Mand 3	-5.86 ± 3.68	-2.55 ± 1.37	0.29 ± 4.77	-0.90 ± 0.49	-2.10 ± 2.03
	Mand 4	-5.49 ± 3.36	-2.41 ± 1.25	0.26 ± 4.44	-0.86 ± 0.46	-1.98 ± 1.82
	Mand 5	-5.14 ± 3.03	-2.29 ± 1.15	0.23 ± 4.12	-0.83 ± 0.44	-1.88 ± 1.60
	Mand 6	-3.99 ± 2.09	-1.72 ± 0.89	0.34 ± 3.10	-0.66 ± 0.33	-1.42 ± 0.98
	Mand 7	-2.72 ± 1.24	-1.05 ± 0.70	0.52 ± 2.04	-0.43 ± 0.21	-0.89 ± 0.44
	All teeth	-2.12 ± 0.94	-0.65 ± 0.64	0.63 ± 1.44	-0.35 ± 0.17	-0.56 ± 0.26
Disc	Mand 1	-0.95 ± 0.55	-4.46 ± 0.97	-2.18 ± 1.12	-2.00 ± 1.27	-0.55 ± 1.64
	Mand 3	-1.01 ± 0.52	-4.14 ± 0.86	-1.96 ± 1.01	-1.87 ± 1.18	-0.63 ± 1.46
	Mand 4	-1.03 ± 0.50	-3.84 ± 0.78	-1.76 ± 0.93	-1.76 ± 1.09	-0.65 ± 1.33
	Mand 5	-1.08 ± 0.48	-3.54 ± 0.69	-1.55 ± 0.84	-1.63 ± 1.00	-0.69 ± 1.18
	Mand 6	-0.93 ± 0.36	-2.55 ± 0.50	-1.01 ± 0.59	-1.20 ± 0.73	-0.61 ± 0.81
	Mand 7	-0.61 ± 0.22	-1.50 ± 0.36	-0.53 ± 0.35	-0.74 ± 0.50	-0.43 ± 0.47
	All teeth	-0.39 ± 0.14	-1.00 ± 0.30	-0.35 ± 0.26	-0.51 ± 0.39	-0.23 ± 0.36
Glenoid fossa	Mand 1	-0.34 ± 0.23	-3.84 ± 2.15	1.31 ± 2.09	-3.36 ± 2.12	-0.68 ± 2.23
	Mand 3	-0.30 ± 0.21	-3.50 ± 2.02	1.16 ± 1.83	-3.07 ± 1.94	-0.61 ± 2.08
	Mand 4	-0.27 ± 0.20	-3.20 ± 1.88	1.04 ± 1.61	-2.81 ± 1.78	-0.56 ± 1.92
	Mand 5	-0.23 ± 0.18	-2.89 ± 1.75	0.91 ± 1.36	-2.55 ± 1.62	-0.51 ± 1.76
	Mand 6	-0.15 ± 0.15	-1.95 ± 1.29	0.60 ± 0.85	-1.76 ± 1.11	-0.17 ± 1.32
	Mand 7	-0.11 ± 0.11	-1.05 ± 0.80	0.33 ± 0.49	-0.98 ± 0.61	0.21 ± 0.90
	All teeth	-0.90 ± 0.09	-0.66 ± 0.55	0.24 ± 0.38	-0.66 ± 0.38	0.36 ± 0.67

degree:KPa

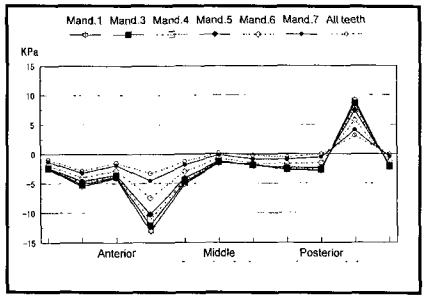

Figure 3A
Nomal stress, sagittal view at condyle

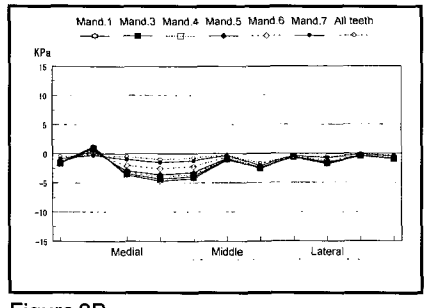

Figure 3B
Nomal stress, frontal view at condyle

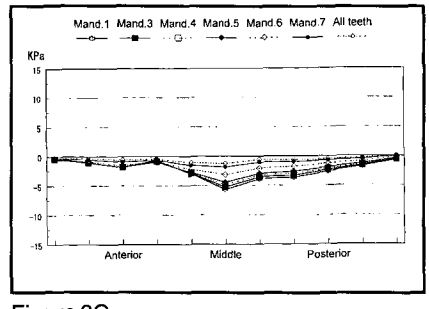

Figure 3C
Nomal stress, sagittal view at disc

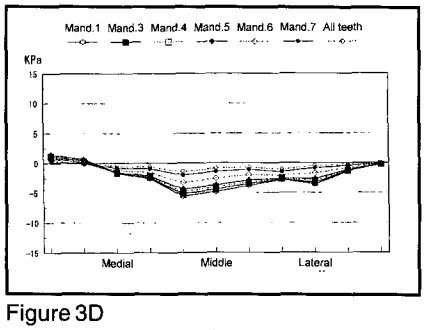

Figure 3D
Nomal stress, frontal view at disc

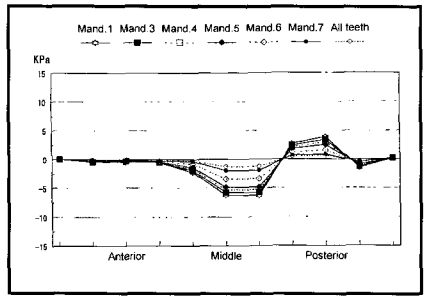

Figure 3E
Nomal stress, sagittal view at glenoid fossa

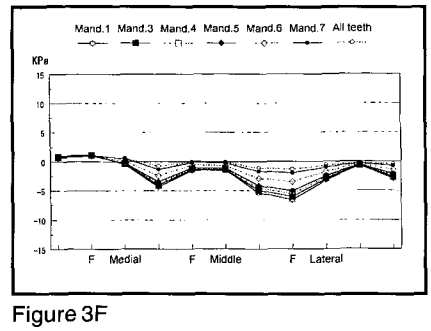

Figure 3F
Nomal stress, frontal view at glenoid fossa

Table 3
Resultant stress distributions at each node

Component	Restraint	Anterior	Middle	Posterior	Lateral	Medial
Condyle	Mand 1	9.78±4.94	8.32±1.56	5.80±3.32	3.33±1.66	4.33±0.91
	Mand 3	8.94±4.48	7.67±1.42	5.44±3.14	3.11±1.48	4.04±0.77
	Mand 4	8.21±4.08	7.09±1.31	5.06±2.92	2.91±1.32	3.73±0.66
	Mand 5	7.50±3.67	6.50±1.18	4.68±2.72	2.72±1.15	3.43±0.55
	Mand 6	5.44±2.54	4.67±0.84	3.48±2.15	2.08±0.75	2.45±0.29
	Mand 7	3.51±1.52	2.86±0.57	2.25±1.59	1.38±0.46	1.51±0.20
	All teeth	2.74±1.15	2.06±0.49	1.69±1.21	1.07±0.41	1.03±0.24
Disc	Mand 1	1.68±0.63	6.67±1.58	2.82±0.67	3.47±2.20	2.41±0.43
	Mand 3	1.62±0.61	6.17±1.39	2.55±0.60	3.20±2.04	2.22±0.40
	Mand 4	1.56±0.58	5.70±1.22	2.31±0.54	2.96±1.90	2.05±0.38
	Mand 5	1.52±0.55	5.25±1.05	2.05±0.48	2.71±1.75	1.88±0.36
	Mand 6	1.20±0.41	3.75±0.63	1.38±0.31	1.93±1.29	1.35±0.29
	Mand 7	0.75±0.25	2.21±0.28	0.78±0.14	1.15±0.85	0.83±0.18
	All teeth	0.49±0.16	1.51±0.18	0.53±0.09	0.80±0.65	0.58±0.10
Glenoid fossa	Mand 1	0.80±0.40	5.08±2.07	4.10±1.46	4.62±2.09	4.08±0.93
	Mand 3	0.75±0.37	4.67±1.94	3.66±1.27	4.22±1.92	3.79±0.89
	Mand 4	0.72±0.33	4.28±1.81	3.29±1.12	3.86±1.76	3.49±0.84
	Mand 5	0.70±0.30	3.89±1.67	2.89±0.96	3.50±1.61	3.20±0.78
	Mand 6	0.59±0.20	2.71±1.19	1.91±0.59	2.40±1.12	2.43±0.57
	Mand 7	0.42±0.11	1.57±0.66	1.08±0.30	1.33±0.62	1.78±0.43
	All teeth	0.30±0.08	1.06±0.41	0.77±0.20	0.87±0.40	1.44±0.41

degree:KPa

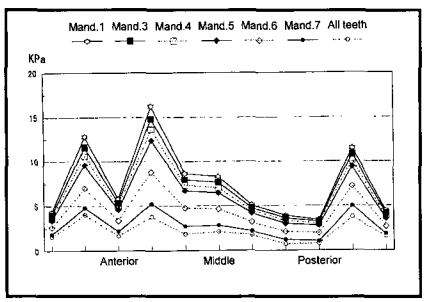

Figure 4A
Resultant stress, sagittal view at condyle

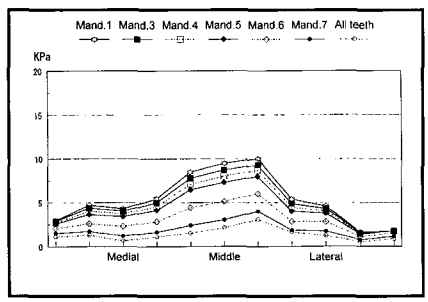

Figure 4B
Resultant stress, frontal view at condyle

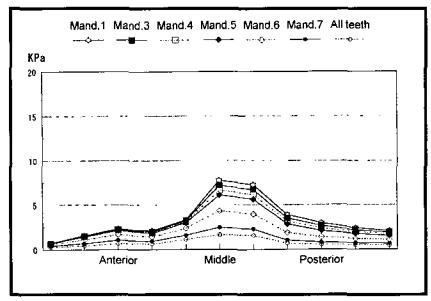

Figure 4C
Resultant stress, sagittal view at disc

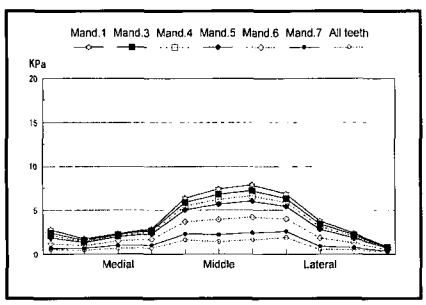

Figure 4D
Resultant stress, frontal view at disc

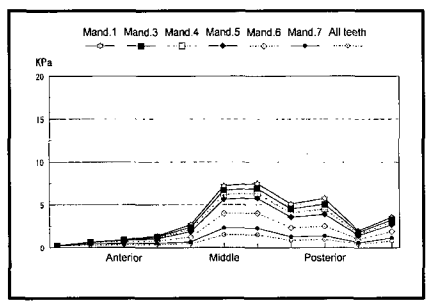

Figure 4E
Resultant stress, sagittal view at glenoid fossa

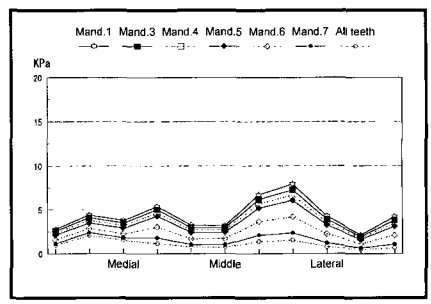

Figure 4F
Resultant stress, frontal view at glenoid fossa

Table 4
Total displacement distributions at each node

Component	Restraint	Anterior	Middle	Posterior	Lateral	Medial
Condyle	Mand 1	0.33±0.01	0.32±0.02	0.32±0.00	0.42±0.03	0.23±0.03
	Mand 3	0.30±0.01	0.29±0.02	0.30±0.00	0.38±0.03	0.22±0.03
	Mand 4	0.28±0.01	0.27±0.01	0.27±0.00	0.35±0.02	0.20±0.03
	Mand 5	0.26±0.01	0.24±0.01	0.24±0.00	0.31±0.02	0.18±0.03
	Mand 6	0.18±0.01	0.17±0.01	0.17±0.00	0.22±0.02	0.13±0.02
	Mand 7	0.10±0.00	0.10±0.00	0.10±0.00	0.12±0.01	0.08±0.01
	All teeth	0.07±0.00	0.07±0.00	0.06±0.00	0.08±0.01	0.06±0.00
Disc	Mand 1	0.11±0.03	0.11±0.06	0.17±0.05	0.23±0.11	0.07±0.04
	Mand 3	0.10±0.03	0.11±0.05	0.15±0.05	0.21±0.10	0.06±0.04
	Mand 4	0.09±0.02	0.10±0.05	0.14±0.04	0.19±0.09	0.06±0.04
	Mand 5	0.08±0.02	0.09±0.05	0.12±0.04	0.17±0.08	0.05±0.03
	Mand 6	0.06±0.02	0.06±0.03	0.08±0.02	0.11±0.05	0.04±0.02
	Mand 7	0.03±0.01	0.04±0.02	0.05±0.01	0.06±0.03	0.02±0.01
	All teeth	0.02±0.01	0.02±0.01	0.03±0.01	0.04±0.02	0.02±0.01
Glenoid fossa	Mand 1	0.00±0.00	0.00±0.00	0.08±0.07	0.00±0.00	0.00±0.00
	Mand 3	0.00±0.00	0.00±0.00	0.07±0.06	0.00±0.00	0.00±0.00
	Mand 4	0.00±0.00	0.00±0.00	0.06±0.05	0.00±0.00	0.00±0.00
	Mand 5	0.00±0.00	0.00±0.00	0.05±0.05	0.00±0.00	0.00±0.00
	Mand 6	0.00±0.00	0.00±0.00	0.03±0.03	0.00±0.00	0.00±0.00
	Mand 7	0.00±0.00	0.00±0.00	0.02±0.02	0.00±0.00	0.00±0.00
	All teeth	0.00±0.00	0.00±0.00	0.01±0.01	0.00±0.00	0.00±0.00

degree:μm

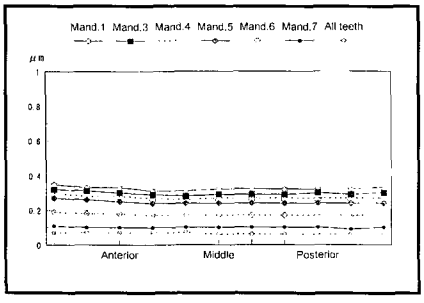

Figure 5A
Total displacement, sagittal view at condyle

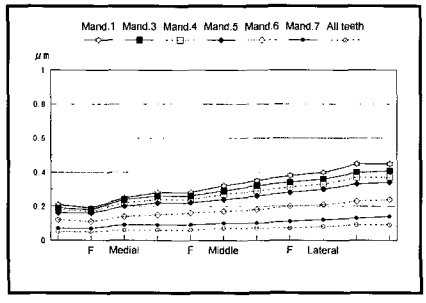

Figure 5B
Total displacement, frontal view at condyle

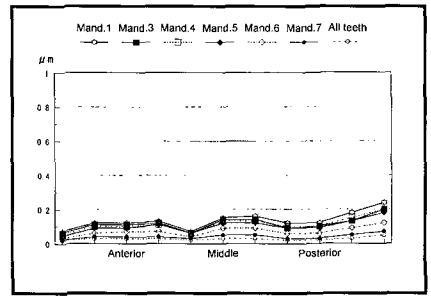

Figure 5C
Total displacement, sagittal view at disc

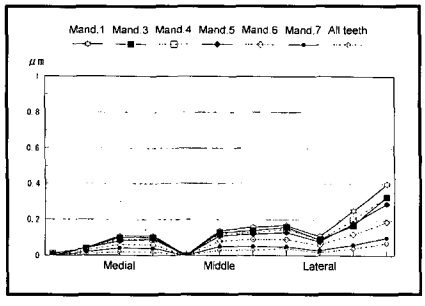

Figure 5D
Total displacement, frontal view at disc

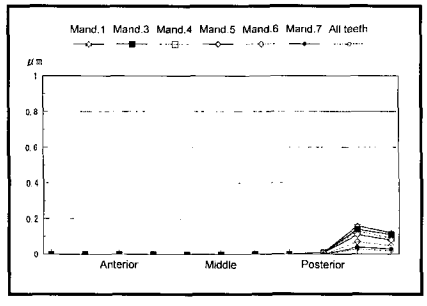

Figure 5E
Total displacement, sagittal view at glenoid fossa

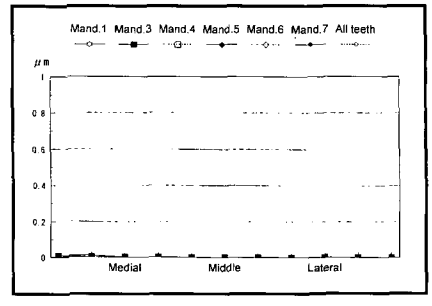

Figure 5F
Total displacement, frontal view at glenoid fossa

4. A symmetrical part should be divided symmetrically.
5. Long, narrow elements should be avoided.

In the present study, and in accordance with the above guidelines, all regions were CT scanned in 2-mm-thick sections, and a three-dimensional finite element model was prepared using 8-node quadrilateral solid elements.

The periodontal ligament is elastic and able to absorb occlusal force, although only up to 100 g of force can be endured; higher loading results in the whole mandible beginning to absorb the force.[19,20] Since the conditions used in the present study relate only to clenching, and the purpose was to investigate the mechanical behavior of the TMJ, the periodontal ligament was not included in our model.

In order to determine the reliability of the finite element analysis, it is essential to compare measurements made on a living human with the calculations obtained using the analysis. However, because of potential damage to the human body when the measurement apparatus is attached to the TMJ, and because of the inconvenient size of the apparatus, measurements in humans are usually limited to intra-articular synovial pressure.

Nitzan et al.[10] reported that synovial pressure of the TMJ is negative during rest, -7.7 + 2.5 mm Hg (-1.03 + 0.33 KPa), and it increases by approximately 20 mm Hg (2.7 KPa) during mastication. Kakudo et al.[11] found that synovial pressure is positive at the intercuspal position, 40.8 mm Hg (5.44 KPa), when using the intracelial pressure of the TMJ during mandibular resting as the standard level.

In practice, describing a small, narrow articular cavity using a three-dimensional finite element model is difficult. Therefore, we assumed that the articular cavity was located at the center of the articular disc, and we focused on the normal stress at this location.

In the present study, normal stress (Table 3) under total tooth restraint conditions—equivalent to a human with normal occlusion—was a compression stress between 0.23 KPa and 1.00 KPa. These values are similar to those obtained by Nitzan et al.,[10] and thus we believe that our model was equivalent to an actual human body.

Results of analyses

Tanaka[8] and Tanaka et al.[13] studied stress distribution in the TMJ during clenching and reported that in the anteroposterior direction, compression stresses were induced in the middle and anterior regions, while tensile stress was produced in the posterior region. Furthermore, in the mediolateral direction, compression stresses were induced in the lateral and middle regions, while tensile stress was produced in the medial region. They also reported that the mean stresses in the mandibular fossa, articular disc, and condylar cartilage were small, approximately one fifth to four fifths of that on the surface of the condyle's compact bone.

In the present study, the results of stress evaluation for each region were similar to those obtained by Tanaka et al.[13]; however, they did not perform displacement analysis. The results of our displacement analysis are summarized below.

Lateral displacement was observed in the most posterior region of the condylar surface, and medial displacements were noted in other regions. Posterior displacement was observed in the medial half of the condylar surface and anterior displacement in the lateral half, starting from the middle region on both sides. Superior displacement was observed in all regions. Medial displacement was observed on the articular disc from the anterior through posterior regions, and lateral displacement was observed in the most lateral and most posterior regions. Posterior displacement was noted in the posterior region, and superior displacement was observed in all regions. Only posterior and superior displacement was noted in the most posterior region of the glenoid fossa surface.

Thus, during clenching, most of the force of the masticatory muscles is absorbed by the teeth, while the rest is withstood by the TMJ. As a result, stress on the surface of the condyle is absorbed by the articular disc, and therefore little displacement occurs on the surface of the glenoid fossa.

A small amount of cancellous bone tissue in the most depressed area is one of the distinct analytical characteristics of the glenoid fossa. Inner and outer cortical bones that come close or join together into a few millimeter-thick part facing the middle cranial fossa in the cranial cavity is another. Therefore, as Hongo[17] reported, the glenoid fossa of the temporal bone protects the brain from harm. The results of the present study depend on the anatomy of the human body.

Resultant displacement and stress were largest when the lower central incisor was restrained, but these values should be considered only from a comparative point of view. Sicher[21] mentioned that overclosure, premature contacts, and mental tension are the most frequent causes of proprioceptive imbalance. Seki,[22] in an epidemiological investigation, reported that the mandible was shifted to the posterior in many TMJ dysfunction cases, and almost all had a deepbite combined with premature incisor contacts. Brandt[23] found that overbite was associated with restricted mandibular opening.

In the present study, we found that premature contact of the incisors was a causative factor of the TMJ disorder, and therefore has important clinical implications.

Conclusions

Biomechanical reaction of the TMJ during clenching was greatest when the lower central incisor was restrained. Premature contact of the lower central incisors may be one of the factors involved in the initiation of temporomandibular arthrosis.

Acknowledgments

We would like to thank Mr. Huruta and Mr. Tokita of Yokogawa Techno-information Service Inc. for their technical assistance.

This work was supported by the Research and Facility Grant for Private Universities and Colleges.

References

1. Hellsing G. Distortion of mandibular kinestesia induced by vibration of human jaw muscles. Scand J Dent Res 1978; 86:486-494.
2. Hansson T, Solberg WK, Penn MK, Oberg T. Anatomic study of TMJs of young adults: A pilot investigation. J Prosthet Dent 1979; 41:556-560.
3. Barghi N, Aguilar T, Martinez C, Woodall WS, Maaskant BA. Prevalence of types of temporomandibular joint clickings in subjects with missing posterior teeth. J Prosthet Dent 1987;57:617-620.
4. Pringle JH. Displacement of the mandibular meniscus and its treatment. Brit J Surg 1981; 6:385-389.
5. Mercuri LG. Intra-articular meniscus dysfunction and the spectrum of TMJ problems. Compend Contin Educ Dent 1985; 6:107-110,113-115.
6. Widmalm SE, Lillie JH, Ash MM. Anatomical and electromyographic studies of the lateral pterygoid muscle. J Oral Rehabil 1987;14:429-446.
7. Haskell B, Day M, Tetz J. Computer-aided modeling in the assessment of the biomechanical determinants of diverse skeletal patterns. Am J Orthod 1986; 89: 363-382.
8. Tanaka E. Stress distributions in the TMJ during clenching. J Osaka Univ Dent Soc 1993; 38:131-160 (in Japanese).
9. Kakudo K, Sugimura T, Suwa F, Fang Y, Shirasu R, Ohta Y. Dynamic responses in the human temporomandibular joint (mandibular fossa) during mandibular movements and changes of mandibular positions. J Jpn Soc TMJ 1995; 7:404-412 (in Japanese).
10. Nitzan DW, Mahler Y, Simkin A. Intra-articular pressure measurements in patients with suddenly developing, severely limited mouth opening. J Oral Maxillofac Surg 1992; 50:1038-1042.
11. Kakudo K, Kotani J, Adachi S, Nakatuji I, Ueda Y, Shirasu R . Intra-articular pressure responses in the human temporomandibular joint during border movements of the mandible (abstract). J Jpn Soc TMJ 1995; 7:197 (in Japanese).
12. Maeda Y, Mori T, Maeda N, Tsutsumi S, Nokubi T, Okuno Y. Biomechanical simulation of the morphological change in the temporomandibular joint. Part 1: Factors influencing stress distribution. J Jpn Soc TMJ 1991; 3:1-9 (in Japanese).
13. Tanaka E, Tanne K, Sakuda M. A three-dimensional finite element model of the mandibule including the TMJ and its application to stress analysis in the TMJ during clenching. Med Eng Phys 1994; 16:316-322.
14. Togawa H. Guide to finite element method. Tokyo: Sience, Co. 1995.
15. Smith GN. An introduction to matrix and finite element methods in civil engineering. London: Applied Science Publishers Ltd, 1971.
16. Smith DM, McLanchlan KR, McCall WD Jr. A numerical model of temporomandibular joint loading. J Dent Res 1986; 65:1046-1052.
17. Hongo T. Quantitative and morphological studies on the trabecular bones in the processus condylaris of the japanese mandibula. Shika Gakuho 1987; 87:1583-1611 (in Japanese).
18. Chen J, Lu X, Paydar N, Akay HU, Roberts WE. Mechanical simulation of the human mandible with and without an endosseous implant. Med Eng Phys 1994;16:53-61.
19. Parfitt GL. Measurement of the physiological mobility of individual teeth in an axial direction. J Dent Res 1960; 39:608-618.
20. Kurashima K. The viscoelastic properties of the periodontal membrane and alveolar bone. J Stomatol Soc Jpn 1963; 30:361-385 (in Japanese).
21. Sicher H. Structural and functional basis for disorders of the temporomandibular articulation. J Oral Surg 1955; 13:275-279.
22. Seki H. Occlusal disharmony in temporomandibular arthrosis viewed from the standpoint of prosthodontics. Part I. Clinical observations. J Stomatol Soc Jpn 1968; 35:213-227 (in Japanese).
23. Brandt D. Temporomandibular disorders and their association with morphologic malocclusion in children. In: Carlson DS, McNamara JA Jr, Ribbens KA, eds. Ann Arbor: The University of Michigan, 1988; 279-298